

Video Transformers under Occlusion: How Physics and Background Attributes Impact Large Models for Robotic Manipulation

Shutong Jin, Ruiyu Wang, Muhammad Zahid and Florian T. Pokorny

Abstract—As transformer architectures and dataset sizes continue to scale, the need to understand the specific dataset factors affecting model performance becomes increasingly urgent. This paper investigates how object physics attributes (color, friction coefficient, shape) and background characteristics (static, dynamic, background complexity) influence the performance of Video Transformers in trajectory prediction tasks under occlusion. Beyond mere occlusion challenges, this study aims to investigate three questions: How do object physics attributes and background characteristics influence the model performance? What kinds of attributes are most influential to the model generalization? Is there a data saturation point for large transformer model performance within a single task? To facilitate this research, we present *OccluManip*, a real-world video-based robot pushing dataset comprising 460,000 consistent recordings of objects with different physics and varying backgrounds. 1.4 TB and in total 1278 hours of high-quality videos of flexible temporal length along with target object trajectories are collected, accommodating tasks with different temporal requirements. Additionally, we propose Video Occlusion Transformer (*VOT*), a generic video-transformer-based network achieving an average 96% accuracy across all 18 sub-datasets provided in *OccluManip*. *OccluManip* and *VOT* will be released at: <https://github.com/ShutongJIN/OccluManip.git>

I. INTRODUCTION

The transformer architecture has established itself as a highly effective tool across a diverse array of sequence-to-sequence problems in natural language processing [1], [2], [3], computer vision [4], [5], [6], decision making [7], [8], [9] and robot manipulation [10], [11], [12]. Among them, video transformers [13], [14], [15] are widely studied for video-based downstream tasks and their ability to effectively capture the complex spatio-temporal relationships and long-range dependencies in video data makes them particularly intriguing for robot perception and planning, e.g., visually-grounded robot manipulation through imitation learning [16], [17], [18], robotic video prediction [19], [20], [21] and goal-conditioned planning with video demonstrations [22], [23], [24]. However, video transformers are computational expensive [25] and their training requires large video datasets [26] that are usually costly to generate on real robots. In the robotic manipulation context, we investigate the impact of physical and background attributes on the performances

The authors are with the School of Electrical Engineering and Computer Science, KTH Royal Institute of Technology shutong@kth.se; fpokorny@kth.se. This work was partially supported by the Wallenberg AI, Autonomous Systems and Software Program (WASP) funded by the Knut and Alice Wallenberg Foundation. The computations were enabled by the supercomputing resource Berzelius provided by National Supercomputer Centre at Linköping University and the Knut and Alice Wallenberg Foundation, Sweden.

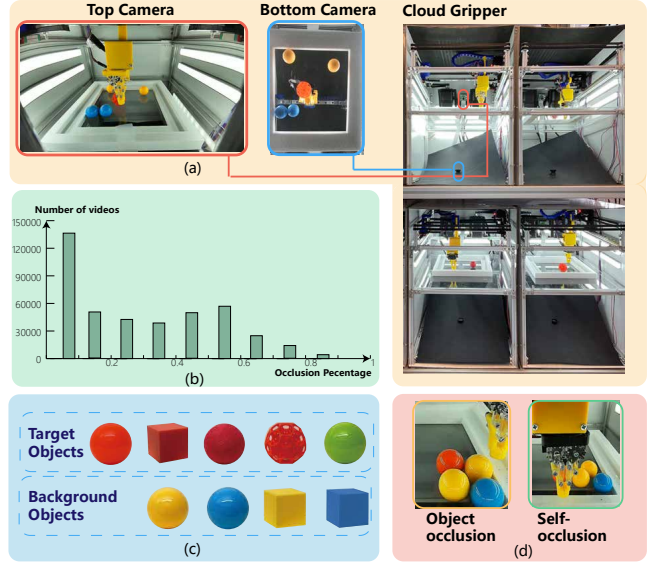


Fig. 1: The dataset, collected with our *CloudGripper* platform - a network of 32 cloud-linked robotic arms, containing robot pushing videos under object and self-occlusion generated from the execution of random planar pushing. (a) The dataset offers RGB videos from both top and bottom cameras. (b) An overview of occlusion percentages across *OccluManip* is also provided. (c) An illustration of target objects and background objects. (d) An example of object occlusion and self-occlusion.

of video transformers to alleviate the burden of model pre-training and provide guidance for real-world data collection.

To tackle this problem, we introduce *OccluManip*, a real-world video-based robot pushing dataset encompassing various objects (*Ball*, *Cube*, *Foam*, *Icosahedron*) with distinct physics attributes (color, friction coefficient, shape) and background settings (static, dynamic, background complexity), resulting in 18 sub-datasets. The combined dataset, collected with our *CloudGripper* system [27], includes 1.4 TB, 460,000 trajectories and 1278 hours of consistent pushing under occlusion videos from a dual-camera system: a top camera view incorporating both self and object occlusion and a bottom camera providing occlusion-free data and precise object location labeling as shown in *Figure. 1 (a)*.

We also present Video Occlusion Transformer (*VOT*), a video-transformer-based network with a generic structure of separate vision and temporal encoding, which takes in the top camera videos with occlusions and predicts a discretized planar positions trace traversed by target object, aligning with the bottom camera view. We refer to this output of grids as a possibility map describing the likely planar positions

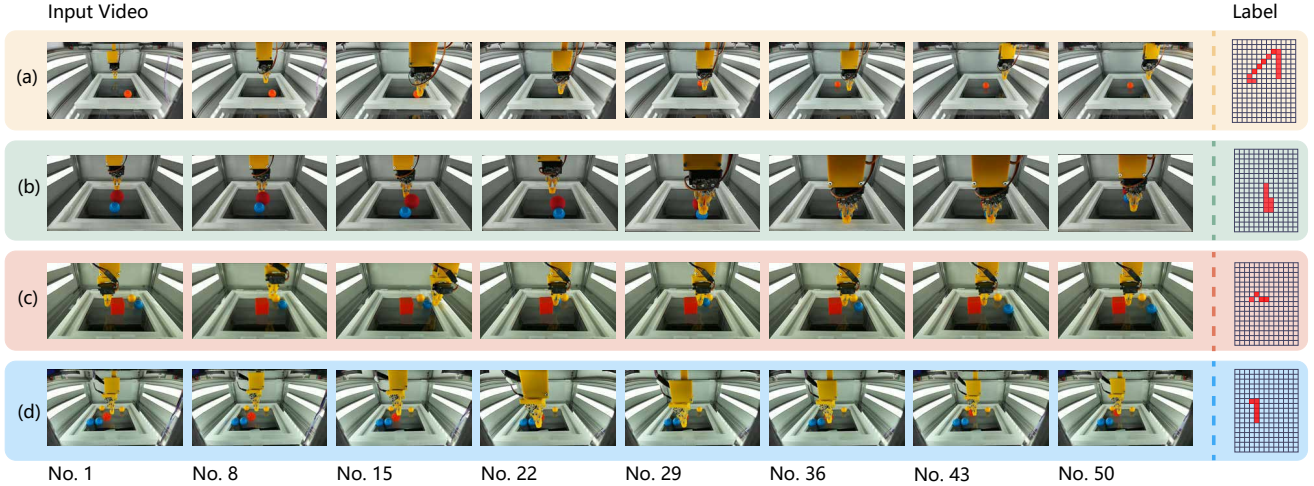


Fig. 2: Selected frames and the according discretized trajectories from *OccluManip* dataset of objects under object and self-occlusion. (a) shows the target object (*Ball*); (b) shows the target object (*Foam*) and one background object; (c) shows the target object (*Cube*) and two background objects; (d) shows the target object (*Icosahedron*) and four background objects.

traced out by the object in the presence of different degrees of occlusion from the top camera perspective. To study the generalisability of video transformers, *VOT* is trained from scratch across all tasks available in *OccluManip*, achieving an average prediction accuracy of 96%. Zero-shot and few-shot learning are conducted for tasks with various physics attributes and background settings. The main contributions of this paper are:

- We propose a large-scale video dataset *OccluManip* with 1278 hours of robot pushing under occlusion which enables the exploration of how physics attributes, background settings and data scale influence the performance of video transformer and other vision-based large models. The dataset is also potentially useful for understanding general occlusion problems and occlusion-aware networks with single camera input, resolving the current request of calibrated RGB-D [28] or multi-camera setups [29].
- A generic video-transformer model *VOT* is designed to predict possibility maps of planar object trajectories discretized into 12×16 grids and with various target objects and changing environmental backgrounds.
- We train *VOT* utilizing all the 18 sub-datasets from scratch and perform zero-shot evaluation and fine-tuning across different sub-datasets, namely. tasks, to bridge the gap in understanding what and how physics attributes and background information influence the performance of video transformers for robotic manipulation.

II. RELATED WORK

A. Model and Dataset Scalability

Despite the transformer architecture's immense potential across various disciplines [3], [5], [12], its quadratic complexity with respect to the number of tokens imposes substantial challenges on both training and data collection [10]. Efforts have been initiated to investigate the scaling behavior, focusing on model size, model depth, dataset size,

computing power and their impact on downstream applications [32], [33], [34], [35]. In the aforementioned works, dataset ablation generally concentrates on the influence of the number of tokens on scaling.

Some endeavors have been made to search for the most effective information to contain during pre-training and essential attributes for achieving meaningful generalization. *Jing et al.* [36] investigated the effects of visual semantics and temporal dynamics on pre-training. In *KitchenShift* [37], the authors crafted a simulated dataset that encompasses 6 factors, such as as lighting and camera pose, to study their impact on imitation learning. *Xie et al.* [38] further extends the factors in *KitchenShift* to 11. However, most of the aforementioned experiments and benchmarks [39], [40] are designed in simulated environments, our dataset *OccluManip* provides large-scale real-world data with a focus on physical attributes (friction coefficient, color and shape) and background characteristics (static, dynamic and background complexity), aiming to provide a useful resource to researchers investigating the impact of these factors with respect to pre-training and fine-tuning models - in particular in the presence of occlusions.

B. Existing Video Datasets

Most the existing video datasets are designed for pure computer vision tasks, such as, action recognition [41], object tracking [42] and video segmentation [43]. Prominent examples include Kinetics400 and Kinetics600 [41], Moments in Time [44], Something-Something V2 (SSv2) [45], AViD [46], Epic Kitchen [47] and Charades[48]. Nonetheless, existing datasets frequently encounter issues like limited size, which can result in overfitting, or restricted video length, and they are not specifically tailored for robotic environments.

Video datasets for robotic manipulation are indeed available, such as, RT-1 [10], HOPE-Video [49], and BC-Z [50]. Nonetheless, owing to the high costs associated with collecting large-scale real-world datasets, the availability of

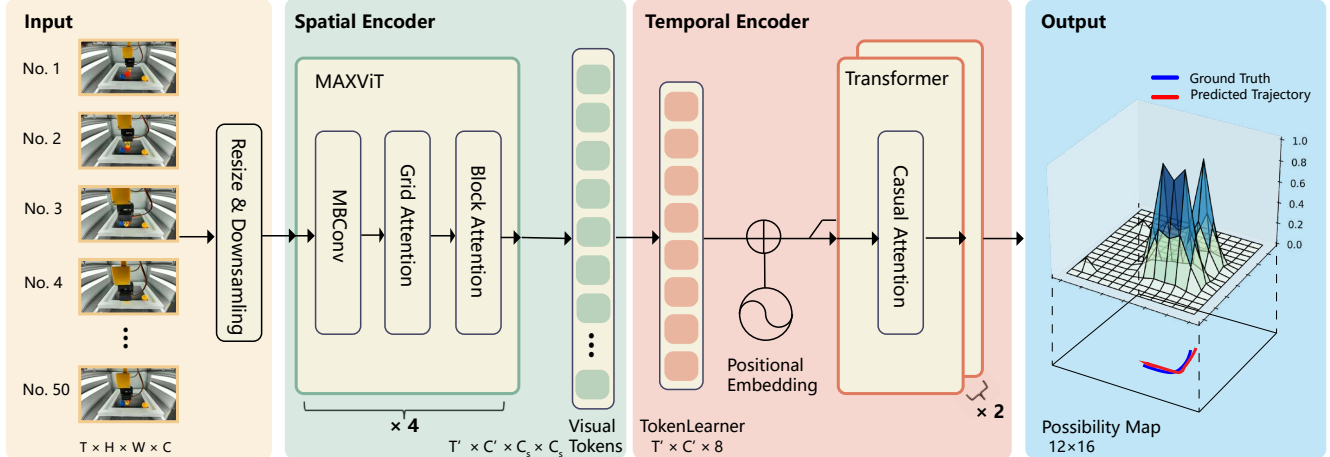


Fig. 3: Model structure. *VOT* intakes top camera videos of T frames, which are resized and downsampled in the first place. Four layers of MaxViT [30] are used as spatial encoder, which generate the encoded visual tokens with C' channels and $C_s \times C_s$ dimension. TokenLearner [31] is adopted to effectively reduce the number of tokens and the reduced tokens go through a 2-layer transformer-based temporal encoder. The final output is a 12 by 16 possibility map, illustrating the possibility of bottom-camera target object trajectories with temporal length T according to the occluded top-camera inputs. Predicted trajectories are generated when the probability within each grid exceeds a specific threshold, e.g. 0.5 in this paper.

video-based robotic manipulation datasets remains relatively limited and not fully open-sourced, in comparison to areas like action recognition. Moreover, a considerable number of these datasets are gathered in simulated environments [51], [52], [53], [54], [55], thereby suffering from the Sim2Real Gap [56]. In this paper, we introduce the *OccluManip*, a real-world video-based robotic pushing dataset comprising 460,000 trajectories, offering a comprehensive occlusion-aware robotic pushing dataset to the community.

C. Video Transformer

Transformers, originally proposed for natural language processing tasks [1], have shown strong capacity when adapted to vision tasks [57], [58]. Video transformers extend the structure of vision transformer [59] by incorporating the temporal dynamics inherent to video data, achieving impressive results in video classification [15], [13], [60], [61], robotic manipulation [10], [28], [62] and object tracking [63], [64], [65].

To address the challenges of computational intensity and rich informational context introduced by the temporal dimension, various factorization methods for spatial and temporal aspects have been employed in recent video transformer architectures. Notably, Swin Video Transformer [13] innovatively adapts the Swin Transformer [5] to include inductive bias, hierarchical structures, and translational invariance, thereby integrating the advantages of CNNs into transformers. ViViT [15] presents several strategies for factorizing both spatial and temporal dimensions to manage the long token sequences often found in video data. VTN [60] utilizes a 2D spatial backbone for feature extraction and employs the Longformer [66] for temporal encoding. In our work, *VOT* adopts the generic structure proposed by VTN [60]. Here, frames are processed through the MaxViT vision transformer [30] to encode spatial features, followed by the application

of the classical Transformer architecture [1] for temporal encoding.

III. DATASET

The *OccluManip* dataset is specifically designed to probe the influence of physical attributes and background characteristics on the generalisability of video transformer. The dataset, obtained via our open cloud-robotics platform, *CloudGripper* [27], provides an extensive collection of 460,000 robot pushing RGB videos varying the object and background attributes, along with precisely-tracked ground-truth object trajectories.

In the *OccluManip* dataset, each Trajectory $Traj = (V_{Top}, V_{Bottom}, P_{Obj}, \xi_{Occ})$ comprises:

- 1) A high-resolution top-camera video V_{Top} of dimension $T \times H_{Top} \times W_{Top} \times C$.
- 2) A corresponding bottom-camera V_{Bottom} of dimension $T \times H_{Bottom} \times W_{Bottom} \times C$.
- 3) Accurate trajectory for the target object in pixel space, $P_{Obj} \in \{(x, y) \mid x, y \in \mathbb{Z}, 0 \leq x \leq 480, 0 \leq y \leq 640\}$.
- 4) Occlusion percentage, $\xi_{Occ} \in \{x \mid x \in \mathbb{R}, 0 \leq x \leq 1\}$.

where $H_{Top}, W_{Top}, H_{Bottom}, W_{Bottom}$ equal to 1280, 720, 480, 640 respectively, standing for the heights and widths of V_{Top} and V_{Bottom} frames; $T = 50$ is the number of frames for each video and $C = 3$ represents the number of video channels, in this case, RGB.

Target object trajectories P_{Obj} are generated from occlusion-free bottom-camera V_{Bottom} , providing precise labels for the top videos containing abundant occlusion.

The *OccluManip* dataset categorizes occlusions during robot pushing into two main types: self-occlusion arising from the gripper and occlusions originating from background objects, one example can be found in Figure. 1 (d). The dataset exhibits four target objects with different physical attributes, including *Ball*, *Cube*, *Foam*, *Icosahedron*. Each

TABLE I: Scratch, Zero-shot and Fine-tuning Performance of *VOT* on *OccluManip* Dataset

	Ball				Cube				Foam				Icosahedron					
	Scratch		Zero-shot		Fine-tune		Scratch		Zero-shot		Fine-tune		Scratch		Zero-shot		Fine-tune	
	Acc	PE	GP	GP	Acc	PE	GP	GP	Acc	PE	GP	GP	Acc	PE	GP	GP		
Single	92.03%	413.1	—	—	98.47%	15.3	—	—	96.93%	61.5	—	—	97.75%	32.9	—	—		
Double	91.13%	512.2	133.6	7.5	96.85%	64.5	190.9	169.9	94.97%	164.5	465.1	624.6	97.46%	41.9	225.0	375.1		
Triple	91.40%	480.7	131.6	242.0	97.74%	33.3	730.4	934.8	95.53%	128.6	443.0	477.2	98.08%	24.8	368.1	67.1		
Quadruple	94.21%	217.8	858.0	637.0	97.93%	28.0	638.8	683.8	97.10%	64.6	232.0	41.0	98.12%	23.1	590.6	201.0		
Quadruple.static	—	—	—	—	—	—	—	—	—	—	—	—	97.85%	23.1	580.3	103.77		

1. "Scratch Accuracy" represents the efficacy of models that are trained end-to-end from scratch, utilizing approximately 20,000 videos.
2. "Zero-shot" refers to the performance of models that are initially trained on the *Single* sub-dataset and subsequently tested on different sub-datasets without further training.
3. "Fine-tuning" describes the process of using the model trained up to the 90th epoch on the *Single* sub-dataset as a pre-trained model. This model is then fine-tuned for an additional 10 epochs using 300 videos from the according sub-dataset.
4. "PE", stands for "Prediction Error", which quantifies the difference between the model's predictions and the actual outcomes.
5. "GP" stands for "Generation Gap", measuring the discrepancy in model performance when transiting between datasets with differing attributes.

TABLE II: Study of Physics Attributes and Background Dynamics

Friction				Shape				Color				Background			
Foam		Ball		Cube		Icosahedron		Ball (Red)		Ball (Green)		Dynamic		Static	
PE	GP	PE	GP	PE	GP	PE	GP	PE	GP	PE	GP	PE	GP	PE	GP
61.5	1032.7	413.4	203.2	15.3	653.5	29.2	611.7	413.7	1098.0	484.9	1509.1	23.1	185.9	30.5	13.0

"PE" here stands for the Prediction Error of the model trained on the original dataset.

"GP" here stands for the Generation Gap when transiting to the other dataset in the same comparing list. For example, $GP_{Foam} = PE_{Foam} - PE_{Ball}$, reflecting the generalisability of transferring model train on *Foam* to *Ball*.

In background study, "Dynamic" and "Static" refers to *Icosahedron Quadruple* and *Icosahedron Quadruple.static* respectively.

of these objects is also captured in different background settings with zero, one, two and four background objects, resulting in a total of 16 sub-datasets. An overview of target and background objects can be seen in *Figure. 1 (c)*. Additionally, two specialized sub-datasets have been created to examine the impact of target object color and background dynamics on video transformers' generalisation ability. Each sub-dataset consists of about 20,000 training and 2,000 testing trajectories. Every video consists of $T = 50$ frames and is recorded at a frame rate of 5 fps. *Figure. 2* exhibits some selected demonstrations of the dataset and *Table. III* outlines the structure, sub-tasks and number of videos in each of the 18 training and testing sub-dataset.

IV. MODEL

The overall design of *VOT* is depicted in *Figure 3*. Our framework is modular in construction which aligns with the generic approach outlined in VTN [60], 2D-spatial backbone with flexible attention-based modules. In *VOT*, the spatial encoder is MaxViT [30], followed by a time encoder employing attention mechanism over temporal domain [1].

Input. The inputs to *VOT* are V_{Top} from top camera in *OccluManip*. We preprocess the input by downsampling it to 25 frames and resizing each frame to 224×224 pixel.

Multi-axis attention. In *VOT*, MaxViT's multi-axis attention mechanism is employed to extract spatial features from each frame. It combines blocked local and dilated global attention, enabling the model to efficiently capture global-local spatial interactions across different input resolutions with linear complexity.

TokenLearner. TokenLearner [31] is used after the spatial encoder to mine the important tokens from the visual data of frames. This step effectively reduces the number of tokens per frame from 8, accelerating the processing further.

Time Encoder. Our Time Encoder is a utilization of classical self-attention mechanism proposed by *Vasawani et al.* [1] to learn the temporal relation between spatial tokens after TokenLearner.

Output The output of the model is a possibility map(ranging from 0 to 1) with dimensions 12×16 , representing the possible trajectory of the target object traversed within temporal length T according to the heavily occluded top-camera inputs.

V. EXPERIMENT

A. Implementation details

Training. We train and evaluate 18 end-to-end *VOT* models on each of the *OccluManip* sub-datasets from scratch, where the sizes of training and testing sets are listed in *Table. III*. The models are diversified by object type (*Ball*, *Cube*, *Foam*, *Icosahedron*) and background complexity (*Single*, *Double*, *Triple*, *Quadruple*). In total, 16 models are formed by combining these factors, along with two additional models, *Quadruple.Static* and *Ball.Green*, to explore other attributes (color, background dynamics). Training is conducted with 8 NVIDIA A100 GPUs on Berzelius [67]. Each model is trained for 100 epochs with a batch size of 4, requiring an estimated 12 hours. We employ the Adam optimizer [68] with constant learning rate of 10^{-4} . The trajectories are discretized into 12×16 grids to serve as labels. All models

TABLE III: Dataset Overview

Object	Background	Training	Testing
Ball (Red)	Single	30030	2800
	Double	22860	1881
	Triple	20720	2570
	Quadruple	20000	1696
Cube	Single	21860	1889
	Double	32870	1500
	Triple	27800	2311
	Quadruple	21610	2180
Foam	Single	19450	2163
	Double	20440	2134
	Triple	20838	2100
	Quadruple	21430	2129
Icosahedron	Single	21670	2697
	Double	24980	2379
	Triple	21430	3150
	Quadruple	22070	1661
	Quadruple_static	25360	3392
Ball (Green)	Single	21540	1660

¹ This table outlines the structure, sub-tasks and number of videos in each of the 18 training and testing sub-dataset.

are randomly initialized and Mean Squared Error (MSE) is adopted as the loss function. The *VOT* model comprises 5×10^7 parameters.

Testing. Each of the 18 testing sub-dataset includes a separate testing set comprising approximately 2,000 videos. All zero-shot experiments are conducted on the testing set, where the same robot is used when collecting the original training set. This ensures that any performance metrics are not influenced by external disturbances unrelated to the attributes under study.

Evaluation Metrics. Three metrics are employed to assess the performance of *VOT*. The Prediction Error (*PE*) quantifies the discrepancy between the predicted and ground-truth trajectories. Accuracy (*Acc*) measures the precision of the trajectory predicted. Finally, the Generation Gap (*GP*) evaluates the model’s generalisability when applied to datasets with different attributes by taking difference of *PE* between the two models.

$$\text{Prediction Error (PE)} = \frac{1}{M \times N} \sum_{i=1}^M \sum_{j=1}^N (R_{ij} - P_{ij})^2 \quad (1)$$

$$\text{Accuracy (Acc)} = 1 - \frac{\sqrt{\text{PE}}}{\text{Scale}}, \quad \text{Acc} \in [0, 1] \quad (2)$$

$$\text{Generation Gap (GP)} = \text{PE}_{\text{new}} - \text{PE}_{\text{previous}} \quad (3)$$

where $M = 12$ and $N = 16$ are the height and width of the predicted possibility grid; P_{ij} ($P_{ij} \in [0, \text{Scale}]$, $\forall i, j$) represents the predicted possibility of object went pass grid (i, j) in each trajectory; R_{ij} ($R_{ij} \in [0, \text{Scale}]$, $\forall i, j$) denotes the discretized ground-truth trajectory; $\text{Scale} = 255$.

B. Experiments of Background Characteristics

Experiments have been performed to investigate the impact of the varying number of background objects, reflecting different levels of background complexity. In this context, “background objects” refer to items present in the scene

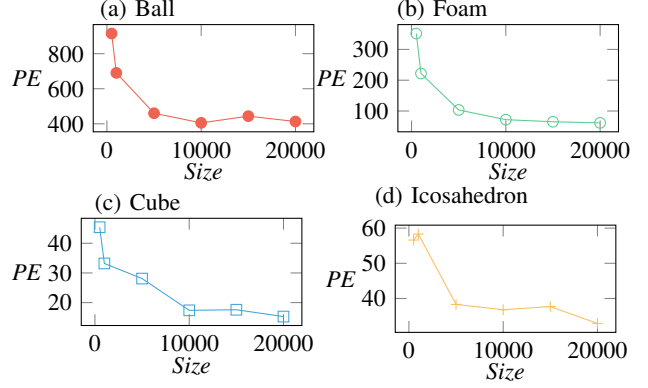


Fig. 4: Saturation Curve of different target objects in *Single* background setting. The x-axis is the size of dataset used for training.

that are not the target object. As outlined in the dataset description and *Table. III*, we increase the number of background objects exponentially: *Single* refers to a scenario with only the target object, *Double* includes one target object and one background object, and so on. An additional test, *Quadruple_Static*, replaces background balls with cubes of the same size and color, which move less frequently compared with balls, to assess the impact of environmental dynamics on model performance. An overview of the types of target objects and background objects is provided in *Figure. 1(c)*.

The experimental results are shown in *Table. I*. The models trained from scratch achieve high accuracy and no significant decrease is observed in performance when the number of objects increases. In the “Zero-shot” columns, *GP* stands for the difference between the zero-shot *PE* and the *PE_{Single}*, revealing the generalisability of models when transferring to settings with multiple background objects. Based on *GP*, we can observe that: (i) the model’s performance is sensitive to the presence of background objects; (ii) in most cases, *GP* increases with the addition of more background objects, although this is not strictly correlated with either their number or complexity; (iii) dynamics of background objects do not make a significant difference, as shown in the cases of *Quadruple* and *Quadruple_Static* for *Icosahedron*.

C. Physical Attributes and Background Dynamics

In *Table. II*, we study the impact of physics attributes on model generalisability by comparing the zero-shot model performance across different single object tasks of 4 groups: *Foam* and *Ball* share identical shape and color but differ significantly in friction coefficients; *Cube* and *Icosahedron* possess the same friction coefficients, given that they are 3D-printed with the same material, and involve only sliding when pushing, therefore are used to estimate the influence of object shape; *Ball* with red and green colors; *Icosahedron* under *Quadruple* and *Quadruple_Static* have the same object and background color, so that the only changing variable is

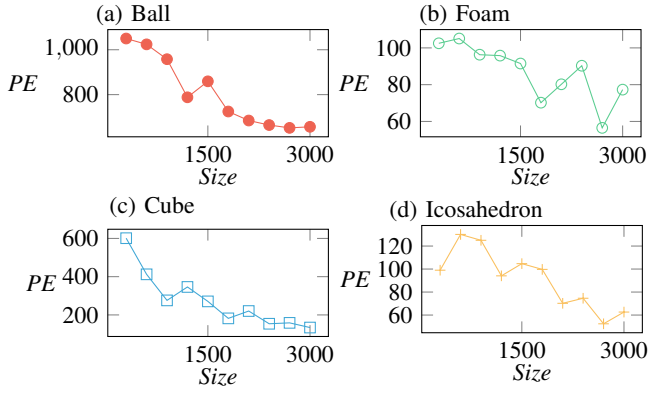


Fig. 5: Models are pre-trained for 90 epochs in the *Single* setting and then fine-tuned and evaluated on a *Quadruple* background setting for 10 epochs. The x-axis represents the fine-tuning dataset size.

the background dynamics.

Table. II presents three key observations: (i) the influence of color is considerably more significant than other attributes such as friction coefficient and shape, and (ii) models trained on balls, which feature in longer and more complicated trajectories, demonstrate better generalization capabilities compared to those trained on foam, which has shorter and relatively simpler trajectories, (iii) the cross experiment on background reinforces the conclusion we draw in background objects dynamics above.

D. Experiment of Saturation Curve

As shown in Figure. 4, we train models for all objects with dataset size of 500, 1000, 10000, 15000, 20000 videos respectively. “Elbow points” in *PE* are identified across four objects, indicating that the performance of transformer architectures may saturate with sufficient data on single tasks. This provides valuable guidance for optimizing resource allocation, reducing the computational overhead of training transformers.

E. Experiment of Fine-Tuning Dataset Size

We investigate the optimal size for fine-tuning datasets by fine-tuning the model with dataset of varying sizes, ranging from 300 to 3000, as shown in Figure. 5. While it is commonly accepted that smaller fine-tuning datasets are preferred to leverage pre-trained models effectively, our results indicate that although prediction error generally decreases with larger dataset sizes, a high degree of variability persists until the dataset reaches a certain threshold size.

F. Discussion

As shown in Figure. 6, (a) illustrates a complex long-range trajectory where the target object collides with the boundary four times. The Video Transformer demonstrates strong inferential capabilities in complex situations that align with its training scenarios. (b) showcases an instance of severe occlusion (90%), yet the Video Transformer maintains

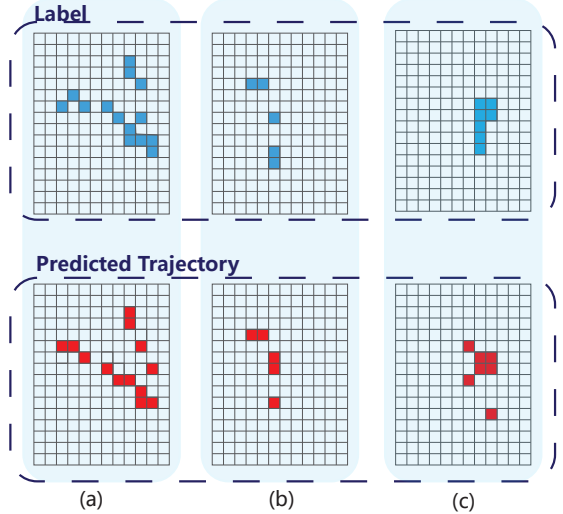


Fig. 6: Examples of predicted and their corresponding ground-truth trajectories. Grids with a possibility larger than 0.5 are recognized as predicted trajectories. (a) An example of a complicated long trajectory. (b) An example of predicted trajectories under 90% occlusion percentage. (c) An example of failure mode. The breaking points in label and predicted trajectory resulted from the down-sampling of input videos.

robust performance. (c) presents a failure mode. In this particular case, due to the target object’s smooth texture (a ball) and potential invisible scratches on the movement plane accumulated from tens of thousands of pushes, the object begins to exhibit self-vibrations. This behavior deviates from the standard movement patterns that the Video Transformer has been trained to recognize.

VI. CONCLUSIONS

In summary, we present *OccluManip*, a robot pushing video dataset featuring diverse physics attributes and background characteristics, alongside *VOT*, a generic video transformer for trajectory prediction under occlusion. The experiments across datasets provide empirical evidence that i) *VOT*’s data saturation starts to become visible at larger training data sizes of around 1000h of training data. ii) *VOT*’s performance is highly sensitive to object color. While not surprising, generalization across object color therefore still poses a challenge for future applications of these architectures to robotics problems that inherently do not depend on color (such as object prediction). iii) We observed that *VOT* performance is furthermore sensitive to the presence of background objects, but no clear trend in how the number or type of objects and their dynamics influence performance could be established. This could be in part due to limitations in spatial resolution of the proposed possibility map as well as data size limitations and will require further investigation. In summary, while promising accuracy results are demonstrated further investigation into the parameter dependence of *VOT* and similar vision transformer based architectures is required in our view before these methods can be reliably deployed in real world robotic manipulation settings.

REFERENCES

[1] A. Vaswani, N. Shazeer, N. Parmar, J. Uszkoreit, L. Jones, A. N. Gomez, L. u. Kaiser, and I. Polosukhin, “Attention is all you need,” in *Advances in Neural Information Processing Systems*, 2017.

[2] A. Radford, J. Wu, R. Child, D. Luan, D. Amodei, and I. Sutskever, “Language models are unsupervised multitask learners,” 2019.

[3] J. Devlin, M.-W. Chang, K. Lee, and K. Toutanova, “BERT: Pre-training of deep bidirectional transformers for language understanding,” in *Conference of the North American Chapter of the Association for Computational Linguistics*, 2019.

[4] A. Dosovitskiy, L. Beyer, A. Kolesnikov, D. Weissenborn, X. Zhai, T. Unterthiner, M. Dehghani, M. Minderer, G. Heigold, S. Gelly, J. Uszkoreit, and N. Houlsby, “An image is worth 16x16 words: Transformers for image recognition at scale,” in *International Conference on Learning Representations*, 2021.

[5] Z. Liu, Y. Lin, Y. Cao, H. Hu, Y. Wei, Z. Zhang, S. Lin, and B. Guo, “Swin transformer: Hierarchical vision transformer using shifted windows,” in *Proceedings of the IEEE/CVF international conference on computer vision*, 2021, pp. 10 012–10 022.

[6] A. Arnab, M. Dehghani, G. Heigold, C. Sun, M. Lučić, and C. Schmid, “Vivit: A video vision transformer,” in *Proceedings of the IEEE/CVF International Conference on Computer Vision (ICCV)*, October 2021, pp. 6836–6846.

[7] L. Chen, K. Lu, A. Rajeswaran, K. Lee, A. Grover, M. Laskin, P. Abbeel, A. Srinivas, and I. Mordatch, “Decision transformer: Reinforcement learning via sequence modeling,” in *Advances in Neural Information Processing Systems*, vol. 34, 2021, pp. 15 084–15 097.

[8] K.-H. Lee, O. Nachum, M. S. Yang, L. Lee, D. Freeman, S. Guadarrama, I. Fischer, W. Xu, E. Jang, H. Michalewski, and I. Mordatch, “Multi-game decision transformers,” in *Advances in Neural Information Processing Systems*, vol. 35, 2022, pp. 27 921–27 936.

[9] Q. Zheng, A. Zhang, and A. Grover, “Online decision transformer,” in *Proceedings of the 39th International Conference on Machine Learning*, ser. Proceedings of Machine Learning Research, vol. 162. PMLR, 17–23 Jul 2022, pp. 27 042–27 059.

[10] A. Brohan, N. Brown, J. Carbajal, Y. Chebotar, J. Dabis, C. Finn, K. Gopalakrishnan, K. Hausman, A. Herzog, J. Hsu *et al.*, “Rt-1: Robotics transformer for real-world control at scale,” *arXiv preprint arXiv:2212.06817*, 2022.

[11] A. Brohan, N. Brown, J. Carbajal, Y. Chebotar, X. Chen, K. Choromanski, T. Ding, D. Driess, A. Dubey, C. Finn, P. Florence, C. Fu, M. G. Arenas, K. Gopalakrishnan, K. Han, K. Hausman, A. Herzog, J. Hsu, B. Ichter, A. Iрpan, N. Joshi, R. Julian, D. Kalashnikov, Y. Kuang, I. Leal, L. Lee, T.-W. E. Lee, S. Levine, Y. Lu, H. Michalewski, I. Mordatch, K. Pertsch, K. Rao, K. Reymann, M. Ryoo, G. Salazar, P. Sanketi, P. Sermanet, J. Singh, A. Singh, R. Soricut, H. Tran, V. Vanhoucke, Q. Vuong, A. Wahid, S. Welker, P. Wohlhart, J. Wu, F. Xia, T. Xiao, P. Xu, S. Xu, T. Yu, and B. Zitkovich, “Rt-2: Vision-language-action models transfer web knowledge to robotic control,” in *arXiv preprint arXiv:2307.15818*, 2023.

[12] M. Shridhar, L. Manuelli, and D. Fox, “Perceiver-actor: A multi-task transformer for robotic manipulation,” in *Proceedings of The 6th Conference on Robot Learning*, ser. Proceedings of Machine Learning Research, K. Liu, D. Kulic, and J. Ichniowski, Eds., vol. 205. PMLR, 14–18 Dec 2023, pp. 785–799.

[13] Z. Liu, J. Ning, Y. Cao, Y. Wei, Z. Zhang, S. Lin, and H. Hu, “Video swin transformer,” in *Proceedings of the IEEE/CVF conference on computer vision and pattern recognition*, 2022, pp. 3202–3211.

[14] M. Patrick, D. Campbell, Y. Asano, I. Misra, F. Metze, C. Feichtenhofer, A. Vedaldi, and J. a. F. Henriques, “Keeping your eye on the ball: Trajectory attention in video transformers,” in *Advances in Neural Information Processing Systems*, M. Ranzato, A. Beygelzimer, Y. Dauphin, P. Liang, and J. W. Vaughan, Eds., vol. 34. Curran Associates, Inc., 2021, pp. 12 493–12 506.

[15] A. Arnab, M. Dehghani, G. Heigold, C. Sun, M. Lučić, and C. Schmid, “Vivit: A video vision transformer,” in *Proceedings of the IEEE/CVF international conference on computer vision*, 2021, pp. 6836–6846.

[16] S. Dasari and A. Gupta, “Transformers for one-shot visual imitation,” in *Proceedings of the 2020 Conference on Robot Learning*, ser. Proceedings of Machine Learning Research, J. Kober, F. Ramos, and C. Tomlin, Eds., vol. 155. PMLR, 16–18 Nov 2021, pp. 2071–2084.

[17] H. Bharadhwaj, A. Gupta, and S. Tulsiani, “Visual affordance prediction for guiding robot exploration,” in *2023 IEEE International Conference on Robotics and Automation (ICRA)*, 2023, pp. 3029–3036.

[18] C. Wang, L. Fan, J. Sun, R. Zhang, L. Fei-Fei, D. Xu, Y. Zhu, and A. Anandkumar, “Minicplay: Long-horizon imitation learning by watching human play,” *arXiv preprint arXiv:2302.12422*, 2023.

[19] R. Rakhimov, D. Volkonskiy, A. Artemov, D. Zorin, and E. Burnaev, “Latent video transformer,” *arXiv preprint arXiv:2006.10704*, 2020.

[20] A. Gupta, S. Tian, Y. Zhang, J. Wu, R. Martín-Martín, and L. Fei-Fei, “Maskvit: Masked visual pre-training for video prediction,” in *The Eleventh International Conference on Learning Representations*, 2023.

[21] C. Nash, J. Carreira, J. C. Walker, I. Barr, A. Jaegle, M. Malinowski, and P. Battaglia, “Transframer: Arbitrary frame prediction with generative models,” *Transactions on Machine Learning Research*, 2023.

[22] J. Sun, D.-A. Huang, B. Lu, Y.-H. Liu, B. Zhou, and A. Garg, “Plate: Visually-grounded planning with transformers in procedural tasks,” *IEEE Robotics and Automation Letters*, vol. 7, no. 2, pp. 4924–4930, 2022.

[23] H. Zhao, I. Hadji, N. Dvornik, K. G. Derpanis, R. P. Wildes, and A. D. Jepson, “P3iv: Probabilistic procedure planning from instructional videos with weak supervision,” in *Proceedings of the IEEE/CVF Conference on Computer Vision and Pattern Recognition*, 2022, pp. 2938–2948.

[24] A.-L. Wang, K.-Y. Lin, J.-R. Du, J. Meng, and W.-S. Zheng, “Event-guided procedure planning from instructional videos with text supervision,” *arXiv preprint arXiv:2308.08885*, 2023.

[25] S. Khan, M. Naseer, M. Hayat, S. W. Zamir, F. S. Khan, and M. Shah, “Transformers in vision: A survey,” *ACM computing surveys (CSUR)*, vol. 54, no. 10s, pp. 1–41, 2022.

[26] Z. Tong, Y. Song, J. Wang, and L. Wang, “VideoMAE: Masked autoencoders are data-efficient learners for self-supervised video pre-training,” in *Advances in Neural Information Processing Systems*, A. H. Oh, A. Agarwal, D. Belgrave, and K. Cho, Eds., 2022.

[27] Z. Muhammad and F. Pokorný, “Cloudgripper - an open cloud-robotics platform,” 2023. [Online]. Available: <https://cloudgripper.org/>

[28] M. Shridhar, L. Manuelli, and D. Fox, “Perceiver-actor: A multi-task transformer for robotic manipulation,” in *Conference on Robot Learning*. PMLR, 2023, pp. 785–799.

[29] ———, “Cliprot: What and where pathways for robotic manipulation,” in *Conference on Robot Learning*. PMLR, 2022, pp. 894–906.

[30] Z. Tu, H. Talebi, H. Zhang, F. Yang, P. Milanfar, A. Bovik, and Y. Li, “Maxvit: Multi-axis vision transformer,” in *European conference on computer vision*. Springer, 2022, pp. 459–479.

[31] M. S. Ryoo, A. Piergiorgianni, A. Arnab, M. Dehghani, and A. Angelova, “Tokenelearner: What can 8 learned tokens do for images and videos?” *arXiv preprint arXiv:2106.11297*, 2021.

[32] Y. Tay, M. Dehghani, J. Rao, W. Fedus, S. Abnar, H. W. Chung, S. Narang, D. Yogatama, A. Vaswani, and D. Metzler, “Scale efficiently: Insights from pre-training and fine-tuning transformers,” *arXiv preprint arXiv:2109.10686*, 2021.

[33] W. Fedus, B. Zoph, and N. Shazeer, “Switch transformers: Scaling to trillion parameter models with simple and efficient sparsity,” *The Journal of Machine Learning Research*, vol. 23, no. 1, pp. 5232–5270, 2022.

[34] Y. Tay, M. Dehghani, S. Abnar, H. W. Chung, W. Fedus, J. Rao, S. Narang, V. Q. Tran, D. Yogatama, and D. Metzler, “Scaling laws vs model architectures: How does inductive bias influence scaling?” *arXiv preprint arXiv:2207.10551*, 2022.

[35] J. Kaplan, S. McCandlish, T. Henighan, T. B. Brown, B. Chess, R. Child, S. Gray, A. Radford, J. Wu, and D. Amodei, “Scaling laws for neural language models,” *arXiv preprint arXiv:2001.08361*, 2020.

[36] Y. Jing, X. Zhu, X. Liu, Q. Sima, T. Yang, Y. Feng, and T. Kong, “Exploring visual pre-training for robot manipulation: Datasets, models and methods,” *arXiv preprint arXiv:2308.03620*, 2023.

[37] E. Xing, A. Gupta, S. Powers, and V. Dean, “Kitchenshift: Evaluating zero-shot generalization of imitation-based policy learning under domain shifts,” in *NeurIPS 2021 Workshop on Distribution Shifts: Connecting Methods and Applications*, 2021.

[38] A. Xie, L. Lee, T. Xiao, and C. Finn, “Decomposing the generalization gap in imitation learning for visual robotic manipulation,” *arXiv preprint arXiv:2307.03659*, 2023.

[39] T. Yu, D. Quillen, Z. He, R. Julian, K. Hausman, C. Finn, and S. Levine, “Meta-world: A benchmark and evaluation for multi-task and meta reinforcement learning,” in *Conference on robot learning*. PMLR, 2020, pp. 1094–1100.

[40] K. Cobbe, C. Hesse, J. Hilton, and J. Schulman, “Leveraging procedural generation to benchmark reinforcement learning,” in *International conference on machine learning*. PMLR, 2020, pp. 2048–2056.

[41] W. Kay, J. Carreira, K. Simonyan, B. Zhang, C. Hillier, S. Vijayanarasimhan, F. Viola, T. Green, T. Back, P. Natsev *et al.*, “The kinetics human action video dataset,” *arXiv preprint arXiv:1705.06950*, 2017.

[42] L. Huang, X. Zhao, and K. Huang, “Got-10k: A large high-diversity benchmark for generic object tracking in the wild,” *IEEE transactions on pattern analysis and machine intelligence*, vol. 43, no. 5, pp. 1562–1577, 2019.

[43] J. Pont-Tuset, F. Perazzi, S. Caelles, P. Arbeláez, A. Sorkine-Hornung, and L. Van Gool, “The 2017 davis challenge on video object segmentation,” *arXiv preprint arXiv:1704.00675*, 2017.

[44] M. Monfort, A. Andonian, B. Zhou, K. Ramakrishnan, S. A. Bargal, T. Yan, L. Brown, Q. Fan, D. Gutfreund, C. Vondrick *et al.*, “Moments in time dataset: one million videos for event understanding,” *IEEE transactions on pattern analysis and machine intelligence*, vol. 42, no. 2, pp. 502–508, 2019.

[45] R. Goyal, S. Ebrahimi Kahou, V. Michalski, J. Materzynska, S. Westphal, H. Kim, V. Haenel, I. Fruend, P. Yianilos, M. Mueller-Freitag *et al.*, “The “something something” video database for learning and evaluating visual common sense,” in *Proceedings of the IEEE international conference on computer vision*, 2017, pp. 5842–5850.

[46] A. Piergiovanni and M. Ryoo, “Avid dataset: Anonymized videos from diverse countries,” *Advances in Neural Information Processing Systems*, vol. 33, pp. 16711–16721, 2020.

[47] D. Damen, H. Doughty, G. M. Farinella, A. Furnari, J. Ma, E. Kazakos, D. Moltisanti, J. Munro, T. Perrett, W. Price, and M. Wray, “Rescaling egocentric vision: Collection, pipeline and challenges for epic-kitchens-100,” *International Journal of Computer Vision (IJCV)*, vol. 130, p. 33–55, 2022.

[48] G. A. Sigurdsson, A. Gupta, C. Schmid, A. Farhadi, and K. Alahari, “Charades-ego: A large-scale dataset of paired third and first person videos,” *arXiv preprint arXiv:1804.09626*, 2018.

[49] S. Tyree, J. Tremblay, T. To, J. Cheng, T. Mosier, J. Smith, and S. Birchfield, “6-dof pose estimation of household objects for robotic manipulation: An accessible dataset and benchmark,” in *International Conference on Intelligent Robots and Systems (IROS)*, 2022.

[50] E. Jang, A. Irpan, M. Khansari, D. Kappler, F. Ebert, C. Lynch, S. Levine, and C. Finn, “Bc-z: Zero-shot task generalization with robotic imitation learning,” in *Conference on Robot Learning*. PMLR, 2022, pp. 991–1002.

[51] A. Mandlekar, D. Xu, J. Wong, S. Nasiriany, C. Wang, R. Kulkarni, L. Fei-Fei, S. Savarese, Y. Zhu, and R. Martín-Martín, “What matters in learning from offline human demonstrations for robot manipulation,” in *5th Annual Conference on Robot Learning*, 2021.

[52] J. Fu, A. Kumar, O. Nachum, G. Tucker, and S. Levine, “D4rl: Datasets for deep data-driven reinforcement learning,” *arXiv preprint arXiv:2004.07219*, 2020.

[53] J. Wong, A. Tung, A. Kurenkov, A. Mandlekar, L. Fei-Fei, S. Savarese, and R. Martín-Martín, “Error-aware imitation learning from teleopera-tion data for mobile manipulation,” in *Conference on Robot Learning*. PMLR, 2022, pp. 1367–1378.

[54] S. James, Z. Ma, D. Rovick Arrojo, and A. J. Davison, “Rlbench: The robot learning benchmark & learning environment,” *IEEE Robotics and Automation Letters*, 2020.

[55] A. Mandlekar, Y. Zhu, A. Garg, J. Booher, M. Spero, A. Tung, J. Gao, J. Emmons, A. Gupta, E. Orbay *et al.*, “Roboturk: A crowdsourcing platform for robotic skill learning through imitation,” in *Conference on Robot Learning*. PMLR, 2018, pp. 879–893.

[56] S. Höfer, K. Bekris, A. Handa, J. C. Gamboa, M. Mozifian, F. Golemo, C. Atkeson, D. Fox, K. Goldberg, J. Leonard *et al.*, “Sim2real in robotics and automation: Applications and challenges,” *IEEE transactions on automation science and engineering*, vol. 18, no. 2, pp. 398–400, 2021.

[57] C.-F. R. Chen, Q. Fan, and R. Panda, “CrossViT: Cross-Attention Multi-Scale Vision Transformer for Image Classification,” in *International Conference on Computer Vision (ICCV)*, 2021.

[58] W. Wang, E. Xie, X. Li, D.-P. Fan, K. Song, D. Liang, T. Lu, P. Luo, and L. Shao, “Pyramid vision transformer: A versatile backbone for dense prediction without convolutions,” in *2021 IEEE/CVF International Conference on Computer Vision (ICCV)*, 2021, pp. 548–558.

[59] A. Dosovitskiy, L. Beyer, A. Kolesnikov, D. Weissenborn, X. Zhai, T. Unterthiner, M. Dehghani, M. Minderer, G. Heigold, S. Gelly *et al.*, “An image is worth 16x16 words: Transformers for image recognition at scale,” *arXiv preprint arXiv:2010.11929*, 2020.

[60] D. Neimark, O. Bar, M. Zohar, and D. Asselmann, “Video transformer network,” in *Proceedings of the IEEE/CVF international conference on computer vision*, 2021, pp. 3163–3172.

[61] G. Bertasius, H. Wang, and L. Torresani, “Is space-time attention all you need for video understanding?” in *ICML*, vol. 2, no. 3, 2021, p. 4.

[62] A. Brohan, N. Brown, J. Carballo, Y. Chebotar, X. Chen, K. Choromanski, T. Ding, D. Driess, A. Dubey, C. Finn *et al.*, “Rt-2: Vision-language-action models transfer web knowledge to robotic control,” *arXiv preprint arXiv:2307.15818*, 2023.

[63] F. Xie, L. Chu, J. Li, Y. Lu, and C. Ma, “Videotrack: Learning to track objects via video transformer,” in *Proceedings of the IEEE/CVF Conference on Computer Vision and Pattern Recognition*, 2023, pp. 22826–22835.

[64] L. Lin, H. Fan, Z. Zhang, Y. Xu, and H. Ling, “Swintrack: A simple and strong baseline for transformer tracking,” *Advances in Neural Information Processing Systems*, vol. 35, pp. 16743–16754, 2022.

[65] N. Wang, W. Zhou, J. Wang, and H. Li, “Transformer meets tracker: Exploiting temporal context for robust visual tracking,” in *Proceedings of the IEEE/CVF conference on computer vision and pattern recognition*, 2021, pp. 1571–1580.

[66] I. Beltagy, M. E. Peters, and A. Cohan, “Longformer: The long-document transformer,” *arXiv preprint arXiv:2004.05150*, 2020.

[67] Berzelius. [Online]. Available: <https://www.nsc.liu.se/systems/berzelius/>

[68] D. P. Kingma and J. Ba, “Adam: A method for stochastic optimization,” *arXiv preprint arXiv:1412.6980*, 2014.